Available online at www.sciencedirect.com
ScienceDirect
Physics Letters A 369 (2007) 333–338
PHYSICS LETTERS A
www.elsevier.com/locate/pla

# Electronic properties of 1D nanographite ribbons in modulated magnetic fields

J.Y. Wu [a], J.H. Ho [a], Y.H. Lai [a], T.S. Li [b], M.F. Lin [a,*]

[a] *Department of Physics, National Cheng Kung University, Taiwan*
[b] *Department of Electrical Engineering, Kun Shan University, Taiwan, Republic of China*

Received 11 April 2007; accepted 26 April 2007

Available online 29 April 2007

Communicated by V.M. Agranovich

**Abstract**

The effects of the modulated magnetic field on one dimension at energy bands of nanographite ribbons are investigated by the Peierls tight-binding model. Electronic properties strongly depend on the strength and the period of the modulated magnetic field, the ribbon width, and the edge structure. The modulated magnetic field could destroy state degeneracy, modify energy dispersions, alter subband spacings, affect wave functions, create additional band-edge states, and cause semiconductor–metal transitions. The main features of energy bands are directly reflected in density of states, such as the number, the positions, the heights, and divergent structures of the prominent peaks.


*PACS:* 71.20.Tx; 73.20.-r; 73.21.-b

*Keywords:* Nanographite ribbon; Modulated magnetic field

A one-dimensional (1D) graphene nanoribbon is a monolayer graphite with a nanoscale width. It can be realized by deposition of nanotubes or diamonds [1–4], cutting [5] mechanically exfoliated graphenes, and patterning epitaxially grown graphenes [6,7]. This new nanoscale carbon materials have attracted a great deal of researches, such as band structure [8], optical absorption spectra [9], and transport properties [10]. Edge structures [11] and ribbon widths [12] significantly influence electronic states and essential physical properties. Two typical ribbons, zigzag and armchair are chosen to be studied; each of them corresponds to evidently different low-energy properties near the Fermi level. The special edge states at the Fermi energy only exist in zigzag ribbons, but not in armchair ribbons. These states have significant influences, for example, on magnetic properties and electron transport. On the other hand, the ribbon width dominates energy gaps of armchair ribbons.

Theoretical calculations predict that the uniform electric and magnetic fields would strongly affect the electronic properties. The former would modify energy dispersions, destroy state degeneracy of energy bands, modulate band gap, and induce semiconductor–metal transitions [9]. The perpendicular uniform magnetic field is also deduced to have intensive effects on the electronic structure [8]. The dispersionless Landau levels are developed while the ribbon width is wide enough to compare with the cyclotron radius. In this Letter, we study the electronic properties of nanographite ribbons which are subject to a spatially modulated magnetic field. The dependence on the period and the strength of the modulated magnetic field is discussed in detail.

* Corresponding author.
*E-mail address:* mflin@mail.ncku.edu.tw (M.F. Lin).

0375-9601/$ – see front matter 
doi:10.1016/j.physleta.2007.04.095

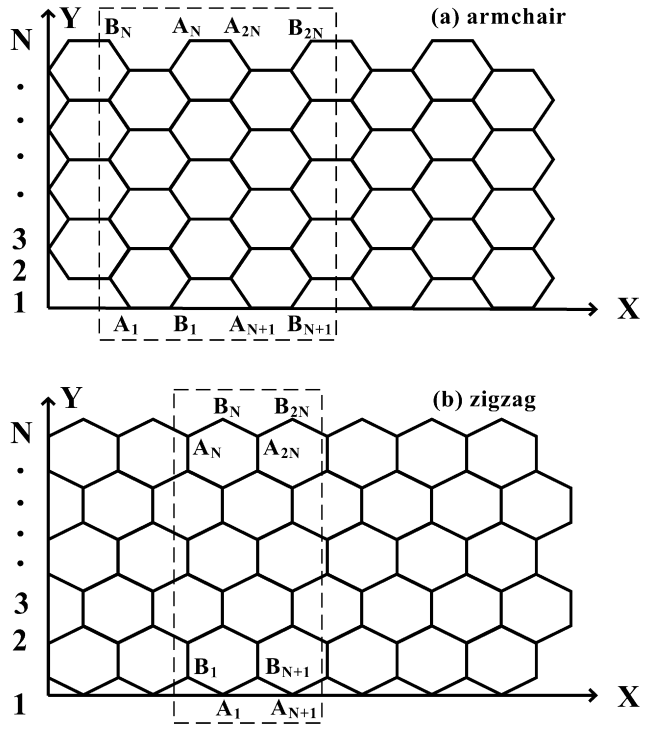


Fig. 1. Nanographite ribbons with (a) armchair edge and (b) zigzag edge. The rectangle with the dashed line is the primitive unit cell in a modulated magnetic field at $R'_B = 2$.

The geometric structure of a 1D nanographite ribbon is shown in Figs. 1(a) and 1(b). In the $x$–$y$ plane, the hexagonal-symmetry carbon atoms form a nanographite ribbon, where atom B is the nearest neighbor for atom A. The C–C bond length is $b = 1.42$ Å. The periodical length along the $x$-axis is $3b(\sqrt{3}\,b)$ for an armchair (a zigzag) ribbon. $N$, the number of dimer lines or zigzag lines along the $y$-axis, denotes the ribbon width. The tight-binding method with the nearest-neighbor interaction $\gamma_0$ is adopted to calculate the low magnetic $\pi$-electronic structures of ribbon systems. An armchair (or a zigzag) ribbon exists in a spatially modulated magnetic field $\mathbf{B} = B' \sin Kx\hat{z}$ perpendicular to the graphite plane. The modulation period along the $x$-axis is $2\pi/K = 3b \cdot R'_B(\sqrt{3}\,b \cdot R'_B)$. The magnetic field would induce the Peierls phase characterized by the vector potential $\mathbf{A} = -B' \cos Kx/K\,\hat{y}$. The nearest-neighbor hopping integral associated with the extra position-dependent phase is

$$\langle b_{j\mathbf{k}}|H_{\mathbf{B}}|a_{i\mathbf{k}}\rangle = \gamma_0 \exp\left\{ i\left[ \mathbf{k}\cdot(\mathbf{R}_i - \mathbf{R}_j) + \frac{2\pi}{\Phi_0}\int_{\mathbf{R}_i}^{\mathbf{R}_j} \mathbf{A}\cdot d\mathbf{r} \right] \right\}. \tag{1}$$

The magnetic modulation period causes the periodical boundary condition along the $x$-axis so that the corresponding Peierls phase is periodic in a period $R'_B$. There are $2N \cdot R'_B$ atoms in a primitive cell. The first Brillouin zone is defined by $\pi/I_x \geqslant k_x \geqslant -\pi/I_x$, where $I_x = 3b \cdot R'_B$ $(\sqrt{3b} \cdot R'_B)$ for an armchair (a zigzag) ribbon. As a result, the Hamiltonian matrix in the presence of a modulated magnetic field is a $2N \cdot R'_B \times 2N \cdot R'_B$ Hermitian matrix. For an armchair ribbon, it could be expressed as

$$H_{lm} = \begin{cases} -\gamma_0 e^{i2\pi\theta_1} e^{ik_x b/2} & \text{if } l = m-3;\ m = 2i+2, \\ -\gamma_0 e^{i2\pi\theta_2} e^{-ik_x b/2} & \text{if } l = 2i;\ m = 2i+1, \\ -\gamma_0 e^{-ik_x b} & \text{if } l = m-1;\ m = 4i, \\ & \text{or } l = 4i-3;\ m = l+1+2N(R'_B-1), \\ -\gamma_0 e^{ik_x b} & \text{if } l = 4i-2;\ m = l-1+2N(R'_B-1). \end{cases} \tag{2}$$

$\theta_1 = [3\Phi' R'^2_B/\pi^2]\cos[\pi(n-1/6)/R'_B]\sin(\pi/6R'_B)$; $\theta_2 = [3\Phi' R'^2_B/\pi^2]\cos[\pi(n+1/2)/R'_B]\sin(\pi/6R'_B)$. The magnetic flux through a hexagon by the $B'$ field, $\Phi' = 3\sqrt{3}\,B'b^2/2\Phi_0$ (in unit of a flux quantum $\Phi_0 = hc/e = 4.1356 \times 10^{-15}\ \mathrm{T\,m^{-2}}$), is used to characterize the strength of the modulated magnetic field.

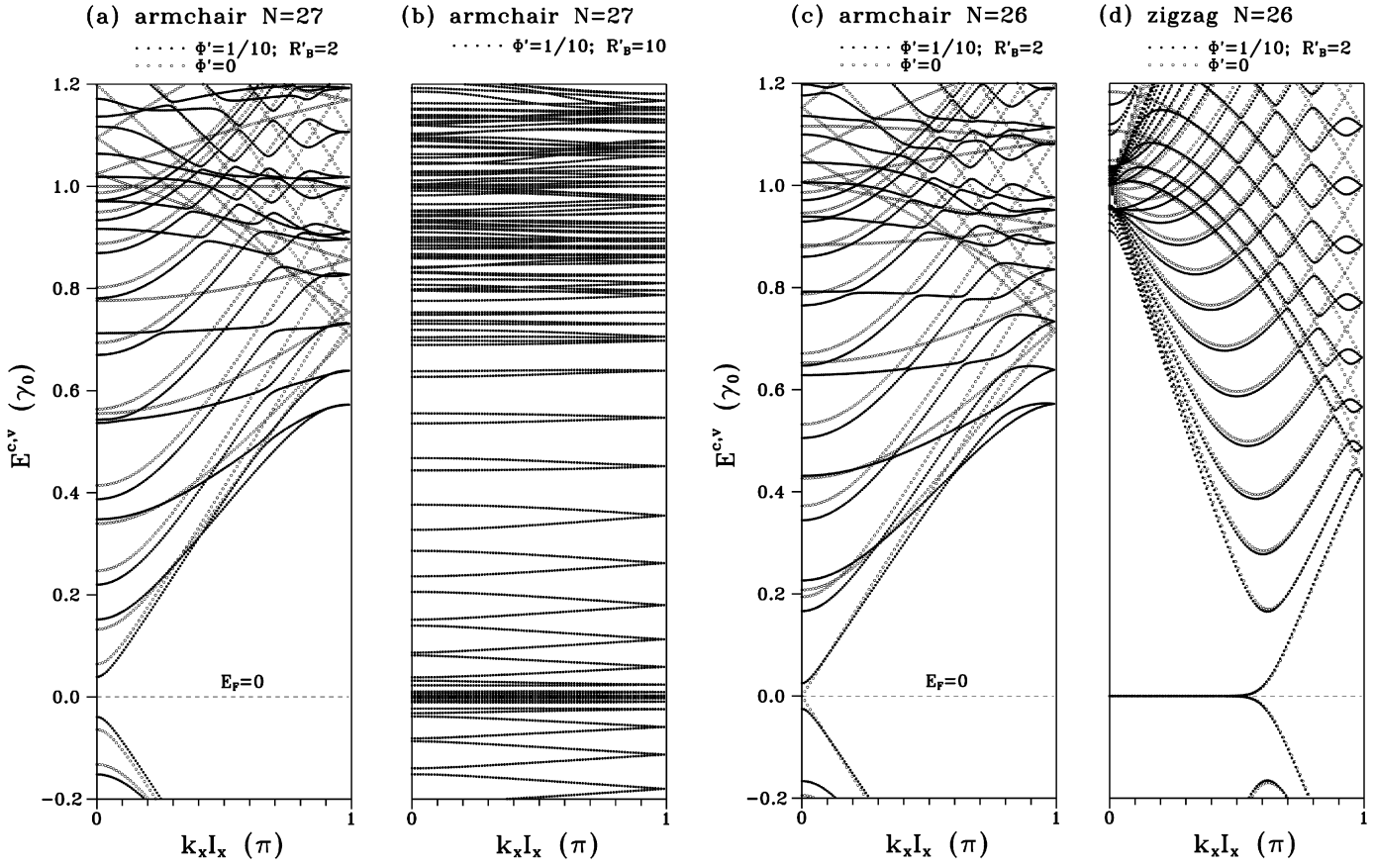


Fig. 2. The low $\pi$-electronic structures of the $N = 27$ armchair ribbon under the modulated magnetic field at different periods: (a) $R'_B = 2$ and $\Phi' = 1/10$; (b) $R'_B = 10$ and $\Phi' = 1/10$. Those at $\Phi' = 1/10$ and $R'_B = 2$ for the (c) $N = 26$ armchair ribbon, and the (d) $N = 26$ zigzag ribbon are also shown. Those without $\Phi'$ correspond to open circles.

As to a zigzag ribbon, the Hamiltonian matrix is given by

$$H_{lm} = \begin{cases} -\gamma_0 e^{i2\pi\theta_1} & \text{if } l = m-3;\ m = 2i+2, \\ -\gamma_0 e^{i2\pi\theta_3} e^{ik_x a/2} & \text{if } l = m-1;\ m = 4i+2, \\ & \text{or } l = 2i+1;\ m = l+2N+1, \\ -\gamma_0 e^{i2\pi\theta_2} e^{-ik_x a/2} & \text{if } l = m-1;\ m = 4i, \\ & \text{or } l = 4i+1;\ m = l+1+2N(R'_B-1), \\ -\gamma_0 e^{ik_x a/2} e^{-i2\pi\theta_3} & \text{if } l = 4i+2;\ m = l+2N-1, \\ -\gamma_0 e^{-ik_x a/2} e^{-i2\pi\theta_2} & \text{if } l = 4i;\ m = l-1+2N(R'_B-1). \end{cases} \tag{3}$$

$\theta_1 = [\Phi' R'^2_B/3\pi^2]\cos[n\pi/R'_B]$, $\theta_2 = [\Phi' R'^2_B/3\pi^2]\cos[\pi(n+1/2)/R'_B]\sin(\pi/2R'_B)$, and $\theta_3 = [\Phi' R'^2_B/3\pi^2]\cos[\pi(n-1/2)/R'_B]\sin(\pi/2R'_B)$. State energy $E^{c,v}$ and wave function $\Psi^{c,v}$ are obtained by diagonalizing the Hamiltonian matrix. The superscript $c(v)$ represents the unoccupied conduction band (the occupied valence band).

The tight-binding model [13] predicts armchair ribbons to be metallic systems for $N = 3I+2$ ($I$ an integer) and semiconductors for others. Zigzag ribbons with partial flat bands which correspond to edge states are always gapless. The $N = 27$, 26 armchair ribbons and $N = 26$ zigzag ribbon, as shown in Figs. 2(a)–2(d), are chosen as three types to be studied. We first see the $N = 27$ armchair ribbon in the absence of the modulated magnetic field (open circles in Fig. 2(a)). The occupied $\pi$ states $E^v(\gamma_0)$ are symmetric to the unoccupied $\pi^*$ states $E^c(\gamma_0)$ with respect to $E_F = 0$, and the symmetry of energy bands remains unchanged under the modulated magnetic field (solid circles). There are complete flat bands at $E = \pm\gamma_0$ and parabolic bands at others. The doubly degenerate complete flat bands are due to $2p_z$ orbitals located at the odd dimer lines, and cause the delta-function-like peaks in DOS. Only the $N = 2I+1$ armchair ribbons have such kind of energy bands. Moreover, the direct energy gap is determined by the $k_x = 0$ state of the parabolic bands.

The modulated magnetic field strongly affects energy bands of armchair ribbons in many aspects: the modification on energy dispersions (band curvatures or effective masses), the creation of extra band-edge states, the destruction of the complete flat bands, the alternation in subband spacings, and the change of energy gap. Fig. 2(a) demonstrates the $N = 27$ armchair ribbon at $R'_B = 2$

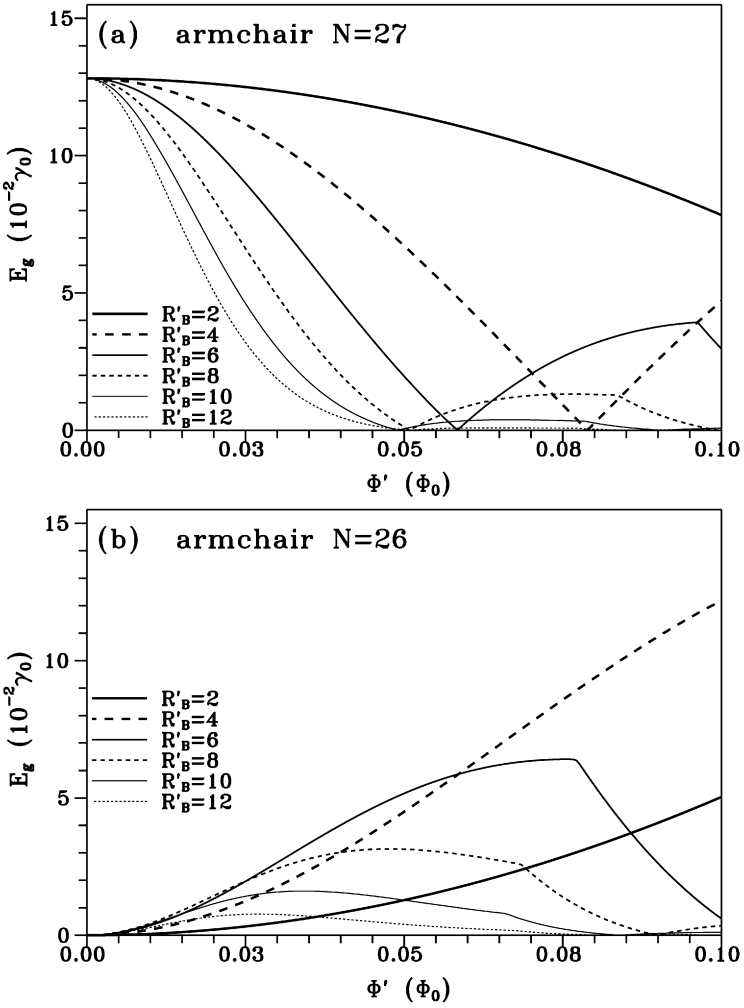


Fig. 3. The magnetic-flux-dependent energy gaps are calculated for the (a) $N = 27$ and (b) $N = 26$ armchair ribbons at different $R'_B$'s.

and $\Phi' = 1/10$. The complete flat bands with double degeneracy at $E^c = \gamma_0$ are changed into two close oscillatory bands beginning at $k_x = 0$ near $E^c = 0.97\gamma_0$. They are the composite energy bands of the oscillating parabolic bands and the partial flat bands; the charges are no longer localized only at the odd dimer lines but also even ones. Also, the linear crossing bands turn into the anticrossing parabolic bands that consist of a concave curve and a convex one, which produces extra band-edge states at $k_x \neq 0$, and the band gap is narrowed when the field is applied. All the above-mentioned features would become apparent when the field strength $\Phi'$ is augmented.

The increment of period has a strong effect on energy bands, as shown in Fig. 2(b) at $R'_B = 10$. Energy gap approaches to zero, since there exist two parabolic bands congregating at the Fermi level. There are more subbands, and energy dispersions are greatly reduced. It can be anticipated that energy bands would be almost dispersionless at large periods ($R'_B \geqslant 1000$). This means that for a sufficiently large period, the modulated magnetic field could transform 1D energy bands into 0D discrete states, or could effectively reduce the dimensionality.

Different ribbon widths and edge shapes under the modulated magnetic field are also discussed. For the $N = 26$ metallic armchair ribbon, the linear bands at $E_F = 0$ are separated into two parabolic bands and a band gap is derived (Fig. 2(c)). The $N = 26$ zigzag ribbon is shown in Fig. 2(d). The highly degenerate states at $E = \gamma_0$ and $k_x = 0$ are destroyed; their energies are roughly divided into two energy regions: $0.91\gamma_0 \leqslant E \leqslant 0.96\gamma_0$ and $\gamma_0 \leqslant E \leqslant 1.04\gamma_0$. The former arises from atoms located at about $1/4$ and $3/4$ on the ribbon width, while the latter are related to the central part. Generally speaking, the energy bands away from $E_F$ are all oscillating parabolic bands. Note that, the partial flat bands at the Fermi level seem to be unchanged, however, the effects on the edge states would become evident at large $R'_B$, which is further discussed in density of states.

The correspondence between the energy gap and the modulated magnetic field is worth a closer study. Fig. 3(a) shows that $E_g$ of the $N = 27$ semiconducting armchair ribbon strongly depends on the field strength and period. Energy gap is reduced by $\Phi'$ and eventually disappears; the metal–semiconductor transition is developed. The field strength further increases, which gives a rise to the oscillatory behavior. Comparing with various periods, the metal–semiconductor transition happens more frequently at large $R'_B$.

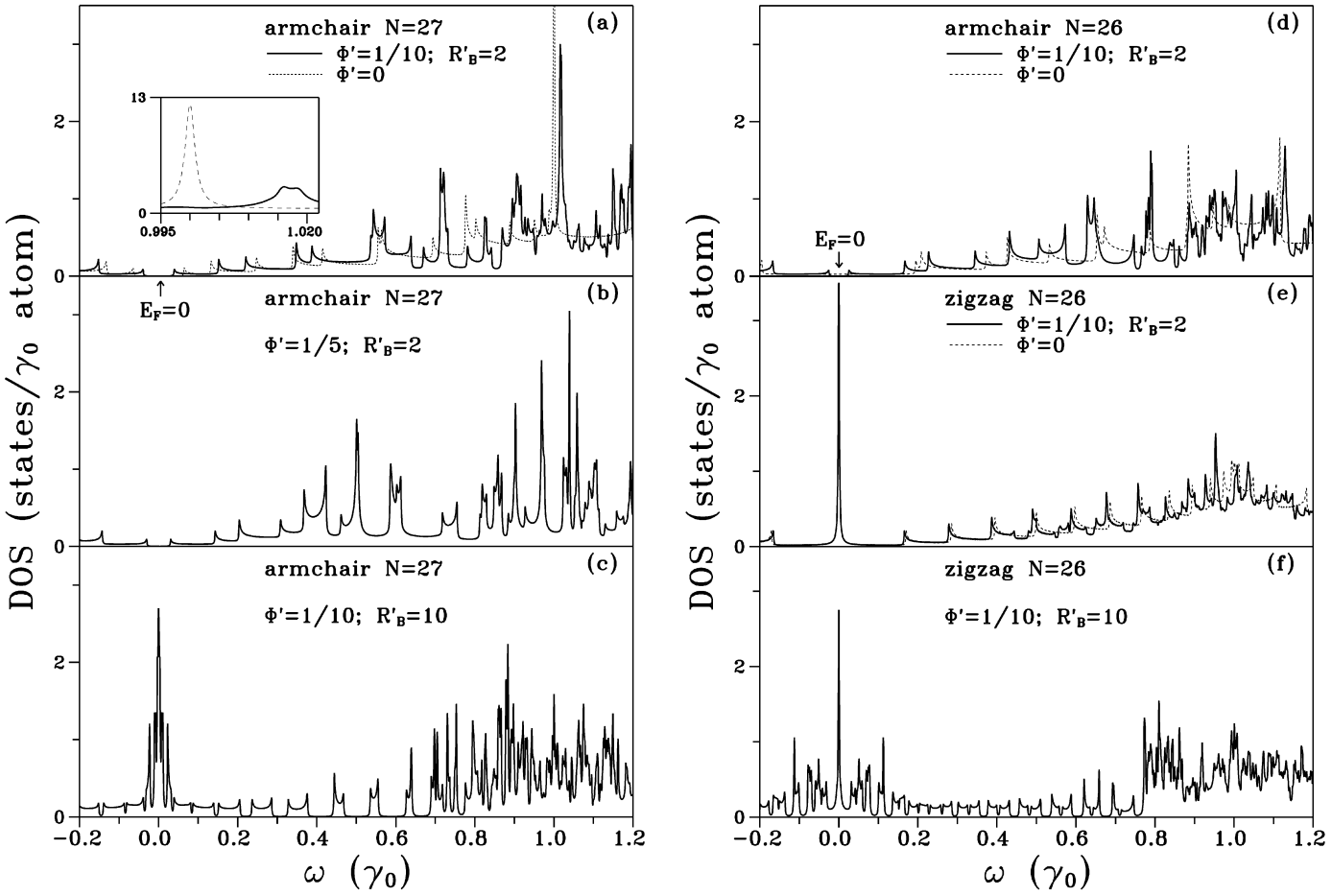


Fig. 4. Density of states for the $N = 27$ armchair ribbon at (a) $\Phi' = 1/10$; $R'_B = 2$, (b) $\Phi' = 1/5$; $R'_B = 2$, and (c) $\Phi' = 1/10$; $R'_B = 10$. Those for (d) the $N = 26$ armchair ribbon at $\Phi' = 1/10$; $R'_B = 2$, (e) the $N = 26$ zigzag ribbon at $\Phi' = 1/10$; $R'_B = 2$, and (f) the $N = 26$ zigzag ribbon at $\Phi' = 1/10$; $R'_B = 10$. Those without $\Phi'$ are also shown in (a), (d) and (e) for comparison. The inset of (a) presents DOS near $\omega = \gamma_0$.

That is to say, the enlargement of $R'_B$ is helpful to this special transition. As to the $N = 26$ metallic armchair ribbon (Fig. 3(b)), its energy gap is easily opened by a very weak magnetic field, i.e., it exhibits the metal–semiconductor transition at $\Phi' \to 0$. $E_g$ first augments with the increasing $\Phi'$, and then begins to drop after a maximal value. The maximum of band gap depending on the period is an oscillatory dispersion relation.

The main characteristics of energy bands are directly reflected in density of states, which is defined as follows:

$$D(\omega) = \frac{2I_x}{2N} \int\limits_{1st\,BZ} \frac{dk_x}{2\pi} \frac{\Gamma}{\pi[(E(k_x) - \omega)^2 + \Gamma^2]}. \tag{4}$$

$\Gamma$ $(= 0.001\gamma_0)$ is the phenomenological broadening parameter. With different ribbon widths and edge structures, DOS exhibits distinct features at the Fermi level. The armchair ribbon has is zero for semiconductor (the dashed curve in Fig. 4(a)), but is non-zero (and small) for metal (Fig. 4(d)), which originates from linear bands along $\hat{k}_x$ (Fig. 2(c)). The zigzag ribbon owns a delta-function-like peak at $E_F = 0$, mainly owning to the special partial flat band. The $N = 27$ armchair ribbon in the absence of the modulated magnetic field exhibits a delta-function-like divergence at $\omega = \gamma_0$ and square-root divergences (Fig. 4(a)). The delta-function-like divergence is caused by the complete flat band, which is absent in $N = 26$ armchair ribbon. The asymmetric divergences are associated with the critical points (the band-edge states) of 1D parabolic bands, which concave upward in conduction bands and concave downward in valence bands. The DOS at these two types of critical points are performed by $D(\omega) \sim 1/\sqrt{\omega - \omega_0}$ and $1/\sqrt{\omega_0 - \omega}$, respectively.

The modulated magnetic fields alter the number, the positions, and the heights of special peaks. In Fig. 4(a), the solid line presents the $N = 27$ armchair ribbon under the modulated magnetic field. There exists some new square-root divergences due to the extra band-edge states, and the two asymmetric peaks near $\omega = 0$ are getting close. The strong delta-function-like divergence at $\omega = \gamma_0$ does not exist; instead there is a pair of asymmetric divergences (inset in Fig. 4(a)), which is caused by two very close composite energy bands (Fig. 2(a)). The effects of the increasing strength are shown in Fig. 4(b). There are more high peaks and the peak spacings are changed. The magnetic field could reduce the band curvatures and thus enhance the peak heights (or the

effective masses). By raising $R'_B$ to 10, band gap is closed with a sharp peak arising at $\omega = 0$ (Fig. 4(c)). Such peak results from the congregation of parabolic conduction and valence bands at $E_F = 0$. The large the field period is, the more the number of asymmetric peaks is. In particular, the delta-function-like peak at $E_F = 0$ in zigzag ribbon becomes lower as $R'_B$ grows (Figs. 4(e)–(f)); that is, the $k_x$-range of partial flat bands is getting narrow. This result means that the distribution of electrons gradually penetrates from the outmost zigzag positions into the inner sites. Apparently, DOS is very sensitive to the changes in ribbon width and edge structure (Figs. 4(a), (d), (e)).

In conclusion, the Peierls tight-binding method is proposed to investigate the effects of the modulated magnetic field on the electronic properties of carbon nanoribbons. Band structures and density of states are mainly determined by the strength and the period of the modulated magnetic field, the ribbon width, and the edge structure. The modulated magnetic fields create extra band-edge states, modify energy dispersions, destroy state degeneracy, affect wave function, alter subband spacings, and induce semiconductor–metal transitions. Most of energy bands are 1D oscillating parabolic dispersions with several band-edge states. The complete flat band with double degeneracy is substituted by two composite energy bands: the superposition of the oscillating parabolic bands and the partial flat bands. The distribution of wave function is no longer by atoms at odd lines but also even ones. The metal–semiconductor transitions only occur in armchair ribbons, and they strongly depend on the ribbon widths. The partial flat bands at $E_F = 0$ in zigzag ribbons could survive for any modulated magnetic field, while the range of wave vector is reduced by the increasing period. Density of states responds directly to the above-mentioned features of energy bands, such as the number, the heights, the frequencies, and the divergent structures of prominent peaks. It exhibits delta-function-like divergences and square-root divergences caused by 0D flat bands and 1D parabolic bands, respectively.

## Acknowledgements

This work was supported by the National Science Council of Taiwan, under the Grant No. NSC 95-2112-M-006-028-MY3.

## References

[1] M. Murakami, S. Iijima, S. Yoshimura, J. Appl. Phys. 60 (1986) 3856.
[2] M. Zhang, D.H. Wu, C.L. Xu, W.K. Wang, Nanostruct. Mater. 10 (1998) 1145.
[3] Y. Shibayama, H. Sato, T. Enoki, M. Endo, Phys. Rev. Lett. 84 (2000) 1744.
[4] A.M. Affoune, B.L.V. Prasad, H. Sato, T. Enoki, Y. Kaburagi, Y. Hishoyama, Chem. Phys. Lett. 348 (2001) 17.
[5] H. Hiura, Appl. Surf. Sci. 222 (2004) 374.
[6] K.S. Novoselov, et al., Nature (London) 438 (2005) 197.
[7] Y. Zhang, Y.W. Tan, H.L. Stormer, P. Kim, Nature (London) 438 (2005) 201.
[8] K. Wakabayashi, M. Fujita, H. Ajiki, M. Sigrist, Phys. Rev. B 59 (1998) 12.
[9] C.P. Chang, Y.C. Huang, C.L. Lu, J.H. Ho, T.S. Li, M.F. Lin, Carbon 44 (2006) 508.
[10] K. Wakabayashi, Phys. Rev. B 64 (2001) 125428.
[11] K. Nakada, M. Fujita, Phys. Rev. B 54 (1996) 24.
[12] M. Ezawa, Phys. Rev. B 73 (2006) 045432.
[13] J.C. Charlier, J.P. Michenaud, X. Gonze, J.P. Vigneron, Phys. Rev. B 44 (1991) 13237.